Vibrational relaxation in the 3 B 1 state of SO2

S. C. Bae, K. Lee, G. H. Kim, and J. K. Ku

Citation: The Journal of Chemical Physics **102**, 1665 (1995); doi: 10.1063/1.468898
View online: http://dx.doi.org/10.1063/1.468898
View Table of Contents: http://scitation.aip.org/content/aip/journal/jcp/102/4?ver=pdfcov
Published by the AIP Publishing

Vibrational relaxation in the $^3B_1$ state of SO_2

S. C. Bae, K. Lee, G. H. Kim, and J. K. Ku
Department of Chemistry, Pohang University of Science and Technology, Pohang, Kyung-buk, 790-784, Korea

(Received 22 August 1994; accepted 21 October 1994)

The vibrational relaxation rate constants of the four low-lying vibrational levels in the $^3B_1$ state of the SO_2 molecule have been investigated by a laser induced phosphorescence method in pure SO_2. The relaxation rate constants for the $^3B_1(0,1,0)$ level have also been studied in Ar, O_2, N_2, and CO_2. The low-lying vibrational levels of the $^3B_1$ state are populated from ground state $SO_2(X\ ^1A_1)$ by direct pumping, and the phosphorescence emissions from the laser excited as well as the collisional product levels are monitored. The state-to-state relaxation rate constants for the upper two levels are assigned by the kinetic simulations of the phosphorescence time profiles observed from each level. The magnitudes of the relaxation rate constants are in the range of $2.3–3.0\times10^{-11}$ $cm^3\,molecule^{-1}\,s^{-1}$ in SO_2 and $0.26–1.3\times10^{-11}$ $cm^3\,molecule^{-1}\,s^{-1}$ in other gases. © *1995 American Institute of Physics.*

I. INTRODUCTION

The spectroscopic and kinetic properties of the low-lying excited states of the SO_2 molecule have drawn substantial interest by several research groups, not only for the intrinsic interest in the physical and chemical properties of the simple triatomic molecule, but also for the practical importance of SO_2 molecules in atmospheric chemistry.[1,2] The absorption spectrum of SO_2 molecules shows three main regions of absorption. The weakest absorption bands appear in the 340–400 nm region. Douglas[3] reported that the upper electronic state responsible for the weakest absorption bands was a triplet state, which was identified as $^3B_1$ by Merer.[4]

It is well known that the $^3B_1$ state of SO_2 has a very long radiative lifetime.[5–10] In addition, it is quite resistant to the physical quenching in collision with other small molecules.[8,9] The radiative lifetimes and quenching rate constants for the $^3B_1$ state of SO_2 by small molecules have been studied most extensively by Calvert and co-workers,[9] although there are many reports by other research groups.[1,5–8,10] Nevertheless, there are no reports of the vibrational relaxation rate constants among the low-lying vibrational levels of the $^3B_1$ state.

In this work, we have generated the four low-lying vibrational levels of the $^3B_1$ state by direct laser excitation from the ground state molecules and investigated the vibrational relaxation rate constants among these low-lying levels. The phosphorescence time profiles from $^3B_1(0,0,0)$ and $^3B_1(0,1,0)$ levels were easily obtained. When the $^3B_1(0,2,0)$ and $^3B_1(1,0,0)$ levels were pumped, the phosphorescence from the laser excited level was weak and disappeared fast, and emissions from $^3B_1(0,1,0)$ and $^3B_1(0,0,0)$ levels appeared with a time delay. The rise and decay profiles of the phosphorescence from the laser excited and collisional product levels enabled us to assign the detailed state-to-state relaxation rate constants among the low-lying vibrational levels of the $^3B_1$ state by kinetic simulations. Schematics of the relevant energy levels in this work are shown in Fig. 1. Recent *ab initio* calculations[11] have shown that other electronic states are not expected to be in this energy range except those high-lying vibrational levels of the ground state, although Brand and co-workers[12] have suggested that the $^3A_2$ state may be located in this energy region.

II. EXPERIMENTAL METHODS

The schematic diagram of the experimental setup is shown in Fig. 2. The cell was made of a 2 l (radius=7.8 cm) Pyrex bulb, and two pairs of 1 in. Pyrex O-ring joints were attached to allow a laser beam path and to connect to the gas handling vacuum rack. The ports for the observation windows were made by attaching 1.5 in. Pyrex tubings to the bulb and cutting the arms with a glass saw as close as possible to the bulb. The SO_2 gas was purchased from Matheson and further purified by the freeze and thaw method and stored in a storage bulb on the vacuum rack. The pressure in the phosphorescence cell above 0.5 Torr was measured using an oil manometer, but a convectron gauge (Phillips 307) was used to measure lower pressures. The convectron gauge was calibrated with a pirani gauge. To study the vibrational relaxation process in the $^3B_1$ state, phosphorescences from the laser excited as well as collisional product levels were monitored at 90° from the laser beam direction through a 0.5 m monochromator (Spex 500M) equipped with a holographic grating and a Hammamatsu R928 photomultiplier (PM) tube. However, the time profiles for measuring the radiative lifetime of the $^3B_1(0,0,0)$ level were directly collected by installing a cutoff filter set in front of the PM tube, since the observation volume in the cell through the monochromator was not enough to neglect the diffusional loss of the excited species at low pressures. The signal from the PM tube was digitized with a transient digitizer (Tektronix 7912HB) and transferred to a laboratory computer for signal averaging and storage for later analysis.

Experiments for pure SO_2 molecules were done in both static and slowly flowing (~0.5 mmoles/min) conditions, and the time profiles were found to be essentially the same. The quenching rate constants for other gases were measured under static conditions keeping the SO_2 pressure at 1.0 Torr. The quenching gases were added directly to the cell and waited for at least 30 min to allow homogeneous mixing in the cell before collecting signals.

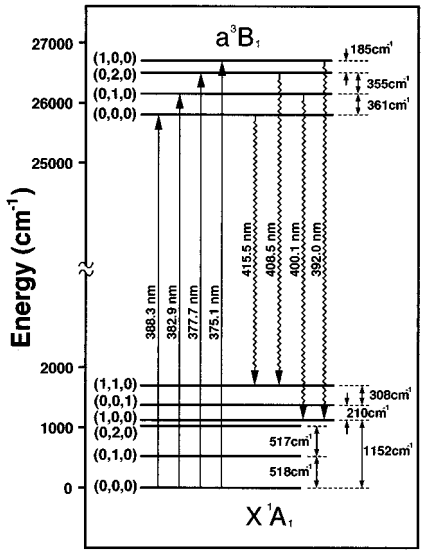

FIG. 1. Schematic energy level diagram for the low-lying vibrational levels of $X\ ^1A_1$ and $a\ ^3B_1$ states relevant to this work. The (0,3,0) level lying 190 cm^{-1} above the (0,0,1) level of the ground state is not shown.

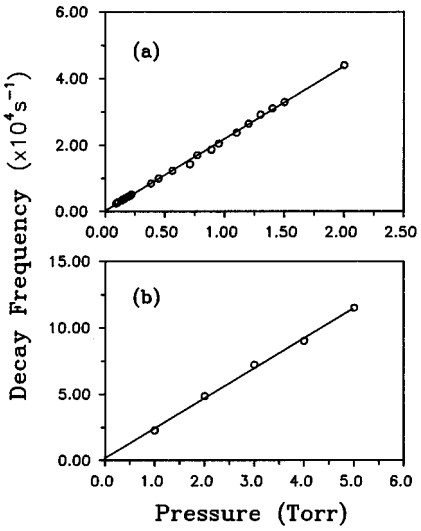

FIG. 3. The pressure dependence of the decay frequencies for the emissions from the $^3B_1(0,0,0)$ level in pure SO_2: (a) was obtained from the emissions with $\lambda \geqslant 400$ nm monitored by installing a cutoff filter set directly in front of the PM tube, and (b) was obtained from monitoring $^3B_1(0,0,0) \rightarrow {}^1A_1(1,1,0)$ emissions centered at 415.5 nm using the monochromator with a 1.1 nm band path. The observation volume in (a) was about 65% of the whole cell volume (2 l bulb), while that in (b) was about 5%.

III. RESULTS

A. Radiative lifetime of the $^3B_1(0,0,0)$ level

The radiative lifetime of the $a\ ^3B_1$ state reported in the literature is widely scattered in the 0.5–10 ms range depending on the experimental method. We have remeasured the radiative lifetime of the $^3B_1(0,0,0)$ level by exciting at 388.3 nm and monitoring the phosphorescence at $\lambda \geqslant 400$ nm using a PM tube with a cutoff filter set. A reliable radiative lifetime is needed to assign the vibrational relaxation rate constants among the low-lying vibrational levels of the $^3B_1$ state. The phosphorescence time profiles from the $^3B_1(0,0,0)$ level showed a single exponential decay. Figure 3(a) shows the Stern–Volmer plot for the $^3B_1(0,0,0)$ level in the 0.1–2.5 Torr range of pure SO_2. The zero pressure intercept extrapolated from the least square fit of the data gives $\tau^0=(8.8\pm2.5)$ ms and the quenching rate constant by SO_2 is $(6.7\pm0.2)\times10^{-13}$ cm^3 $molecule^{-1}$ s^{-1}. The radiative lifetime and the quenching rate constant obtained in this work are in good agreement with those reported by Calvert and co-workers.[9(a)]

Shown in Fig. 3(b) is the Stern–Volmer plot obtained from $X\ ^1A_1(1,1,0) \leftarrow {}^3B_1(0,0,0)$ emissions at 415.5 nm monitored through the monochromator for comparison. The slope of this plot is $(6.9\pm0.2)\times10^{-13}$ cm^3 $molecule^{-1}$ s^{-1}, which is essentially the same as that obtained from Fig. 3(a). However, the zero pressure intercept gives (0.6 ± 0.1) ms as the effective lifetime of the $^3B_1(0,0,0)$ level for this geometry of observation. The observation volume in this geometry is the conical volume with a 1.2 cm radius at the laser beam path. This apparent shortening of the effective lifetime is undoubtedly due to the small observation volume as well as the reduced signal intensities caused by the narrow band path. Because of its long radiative lifetime, some of the excited molecules in the $^3B_1(0,0,0)$ level may diffuse out of the small observation region as reported by several groups.[8(a),9,10] Moreover, the emissions monitored through the monochromator with the 1.1 nm band path are much weaker than the ones monitored using the filter set, and those weak signals, at a later time, may not be effectively detected by a transient digitizer. These phenomena cause a serious problem in determining the true radiative lifetimes of long lived species at low pressures and the radiative lifetime measurements for the $^3B_1$ state of SO_2 provide a good example.

Nevertheless, the collisional quenching rate constants can be determined by the Stern–Volmer analysis for those time profiles monitored with the monochromator without introducing significant errors in spite of the small observation volume used. Since the diffusional loss of the excited molecules out of the observation region depends on the pressure, one can effectively confine excited molecules within a small

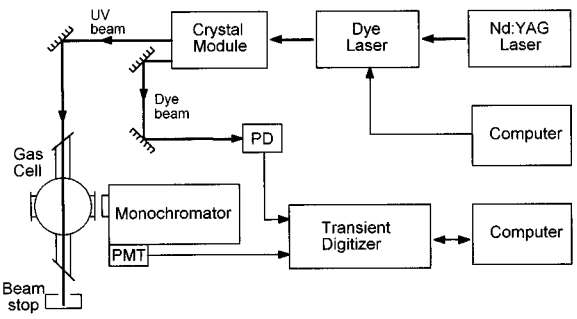

FIG. 2. Schematic diagram of the experimental setup.

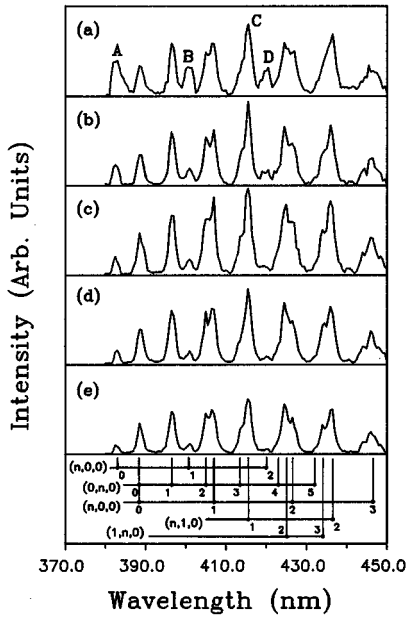

FIG. 4. Low resolution time resolved spectra taken from the $^3B_1(0,1,0)$ level excitation at 382.9 nm: (a) 0.05–0.55, (b) 0.55–1.05, (c) 1.05–2.05, (d) 2.05–4.05, and (e) 4.05–6.05 μs periods. The pressure was 5.0 Torr of pure SO_2 and the slit width was 500 μm. The signal for the initial 0.05 μs was not collected because of the strong scattered laser light at the excitation wavelength. Those peaks indicated as *A*, *B*, and *D* represent $^3B_1(0,1,0)\rightarrow{}^1A_1(n,0,0)$ bands ($n=0$, 1, and 2), respectively, and all the other peaks come from the $^3B_1(0,0,0)\rightarrow{}^1A_1(\nu_1,\nu_2,\nu_3)$ transitions. The peak denoted as *C* is the $^3B_1(0,0,0)\rightarrow{}^1A_1(1,1,0)$ band. (c)–(e) were drawn by multiplying $\frac{1}{2}$, $\frac{1}{4}$, and $\frac{1}{4}$ to the experimental data to correct the different time intervals.

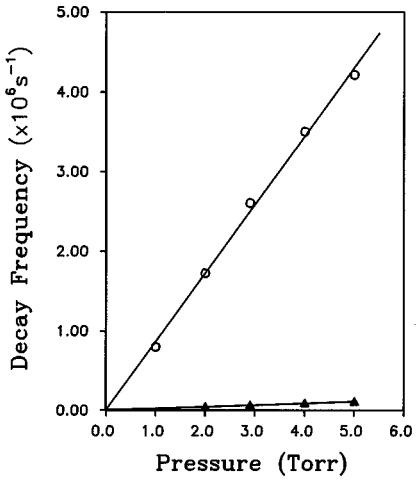

FIG. 5. The pressure dependence of decay constants for the $^3B_1(0,1,0)\rightarrow{}^1A_1(1,0,0)$ emissions. Both fast (○–○) and slow (▲–▲) components are plotted.

volume for a while by choosing an appropriate pressure range. Calvert and co-workers[13] have estimated that the diffusion constant (D) for gaseous SO_2 at 25 °C is $\sim 7.9\times10^4$ $cm^2\ s^{-1}/p$, where p is in the units of mTorr. Since the time t required for a molecule to diffuse a distance x is given approximately by $t=x^2/D$, it will take ~18–90 ms for those excited molecules at the center of the observation volume to diffuse out of the zone at 1.0–5.0 Torr of pressure. Thus the contribution of molecular diffusion to the overall decay rate should be small in the pressure range plotted in Fig. 3(b). The slightly upward movement of the decay constants compared to Fig. 3(a) could be ascribed to the inefficient detection of extremely weak signals at a later time.

B. Time resolved spectra

Typical time resolved spectra from the $^3B_1(0,1,0)$ level excitation at 5.0 Torr of SO_2 are shown in Fig. 4. Those peaks identified in the figure are based on the results from Brand and co-workers,[12] Hochstrasser and Marchetti,[14] and Carter *et al.*[15] The time delay between the laser pulse and the starting point of signal collection was set 50 ns to avoid the effect of scattered laser light at the laser excitation wavelength, and phosphorescence signals from arbitrarily divided ranges were collected. It is clearly seen that the intensities of the $X\ ^1A_1(n,0,0)\leftarrow{}^3B_1(0,1,0)$ bands ($n=0$, 1, and 2; denoted *A*, *B*, and *D*) centered at 382.9, 400.1, and 420.0 nm, respectively, decrease with time, while those of $X\ ^1A_1(v_1,v_2,v_3)\leftarrow{}^3B_1(0,0,0)$ bands (including *C*) increase during the initial 2 μs then decrease with time. The $X\ ^1A_1(1,0,0)\leftarrow{}^3B_1(0,1,0)$ band at 400.1 nm is not only far from the resonance band with a relatively strong intensity, but also well separated from the $X\ ^1A_1(v_1,v_2,v_3)\leftarrow{}^3B_1(0,0,0)$ bands. Thus, the phosphorescence from this band is appropriate to monitor the time behavior of the $^3B_1(0,1,0)$ level. On the other hand, the population change of the $^3B_1(0,0,0)$ level can be monitored at 415.5 nm since the $X\ ^1A_1(1,1,0)\leftarrow{}^3B_1(0,0,0)$ band is far from the excitation wavelength with the strongest intensity. Time resolved spectra taken from exciting the $^3B_1(0,2,0)$ level at 377.7 nm and the $^3B_1(1,0,0)$ level at 375.0 nm, respectively, exhibited very similar features to those shown in Fig. 4. However, those time resolved spectra showed weak but well separated bands from $X\ ^1A_1(1,1,0)\leftarrow{}^3B_1(0,2,0)$ emissions at 408.5 nm and from $X\ ^1A_1(1,0,0)\leftarrow{}^3B_1(1,0,0)$ emissions at 392.0 nm, respectively, at early time, which enabled us to look at the time behavior of the molecules in these levels.

C. Vibrational relaxation rate constant for the $^3B_1(0,1,0)$ level in SO_2

When the $^3B_1(0,1,0)$ level was pumped at 382.9 nm, the phosphorescences from the laser excited level as well as from the $^3B_1(0,0,0)$ level were observed, but the latter appeared with a time delay. The phosphorescence time profiles from the laser excited level clearly showed a double exponential decay. The pressure dependence of the decay frequencies of the fast and slow components is plotted in Fig. 5, and the apparent quenching rate constants are shown in Table I. It is noteworthy that the apparent quenching rate constant for the slow component is essentially the same as that for the $^3B_1(0,0,0)$ level, while that for the fast component is about 40 times larger. Furthermore, the zero pressure intercepts for both components are (0.6 ± 0.1) ms, which are very similar to the effective lifetime of the $^3B_1(0,0,0)$ level observed by us-

TABLE I. Quenching rate constants of $a\ ^3B_1$ state of SO_2 by some quenching gases.

Level	Quenching gases	Rate constants ($cm^3\ molecule^{-1}\ s^{-1}$) This work	Others ($\times 10^{-13}$)
$^3B_1(0,0,0)$	SO_2	$6.7 \pm 0.2\times10^{-13}$	7.51±0.30;[a] 6.8;[b] 7.0±0.2;[c] 6.5±0.2;[d] 6.1;[e] 7.4±0.2;[f] 0.42±0.08[g]
	Ar	$5.8 \pm 0.3\times10^{-14}$	0.55;[f] 0.86[h]
	N_2	$1.2 \pm 0.1\times10^{-13}$	1.4[h]
	O_2	$1.1 \pm 0.1\times10^{-13}$	1.6[h]
	CO_2	$2.1 \pm 0.1\times10^{-13}$	1.9[h]
$^3B_1(0,1,0)$	SO_2 (F)	$2.7 \pm 0.1\times10^{-11}$	
	(S)	$6.8 \pm 0.3\times10^{-13}$	
	Ar (F)	$3.0 \pm 0.1\times10^{-12}$	
	(S)	$4 \pm 2\times10^{-14}$	
	N_2 (F)	$5.9 \pm 0.2\times10^{-12}$	
	(S)	$1.1 \pm 0.2\times10^{-13}$	
	O_2 (F)	$5.6 \pm 0.1\times10^{-12}$	
	(S)	$1.0 \pm 0.3\times10^{-13}$	
	CO_2 (F)	$1.5 \pm 0.1\times10^{-11}$	
	(S)	$2.3 \pm 0.3\times10^{-13}$	
$^3B_1(0,2,0)$	SO_2	$2.8 \pm 0.2\times10^{-11}$	
$^3B_1(1,0,0)$	SO_2	$3.0 \pm 0.1\times10^{-11}$	
τ^0 for (0,0,0) level (ms)		8.8 ± 2.5	0.89±0.13;[a] 8.1±2.5;[c] 1.02±0.71[d] 0.88±0.14;[e] 100±60;[g] 7±1;[i] 0.76±0.16;[j] 0.2[k]

[a]Reference 8(a).
[b]Reference 8(b).
[c]Reference 9(a).
[d]Reference 9(d).
[e]Reference 9(e).
[f]Reference 10.
[g]Reference 9(f).
[h]Reference 9(c).
[i]Reference 7.
[j]Reference 6.
[k]Reference 5.

ing the monochromator. Since the quenching rate constant for the $^3B_1(0,0,0)$ level by SO_2 is very small, that for the $^3B_1(0,1,0)$ level lying only 361 cm^{-1} above the $^3B_1(0,0,0)$ level is not expected to increase dramatically. Thus, the large apparent quenching rate constant for the fast component of the $^3B_1(0,1,0)$ level observed in this work must be related to the fast vibrational relaxation process. This is also supported by the strong emissions from the $^3B_1(0,0,0)$ level which appeared with a time delay.

We have attempted to find out the magnitude of the vibrational relaxation rate constants by fitting this system to the well-known three-level kinetic scheme,[16,17] which is described by

$$\begin{array}{ccc} A = {}^3B_1(0,1,0) & \underset{K_{-2}}{\overset{K_2}{\rightleftarrows}} & {}^3B_1(0,0,0) = B \\ K_1 \downarrow & & K_3 \downarrow \\ & X\ {}^1A_1, & \end{array}$$

$K_1 = 1/\tau_1 + k^{Q1}[SO_2]$,

$K_2 = k^{10}[SO_2]$,

$K_{-2} = k^{01}[SO_2]$,

$K_3 = 1/\tau_0 + k^{Q0}[SO_2]$,

τ_1 = radiative lifetime for $^3B_1(0,1,0)$, (1)

τ_0 = radiative lifetime for $^3B_1(0,0,0)$,

k^{Q1} = quenching rate constant for $^3B_1(0,1,0)$ by SO_2,

k^{Q0} = quenching rate constant for $^3B_1(0,0,0)$ by SO_2,

k^{10} = vibrational relaxation rate constant from $(0,1,0)$ to $(0,0,0)$,

k^{01} = vibrational mixing rate constant from $(0,0,0)$ to $(0,1,0)$.

The coupled differential equations for the above scheme can be written as

$$\begin{aligned} \frac{d[A]}{dt} &= -(K_1+K_2)[A] + K_{-2}[B], \\ \frac{d[B]}{dt} &= K_2[A] - (K_{-2}+K_3)[B]. \end{aligned} \tag{2}$$

The standard solution to the equations is

$$\begin{aligned} [A(t)] &= [A(0)](\lambda_+ - \lambda_-)^{-1}[(\lambda_- + K_1 + K_2)e^{-\lambda_+ t} \\ &\quad + (\lambda_+ - K_1 - K_2)e^{-\lambda_- t}], \\ [B(t)] &= [A(0)]K_2(\lambda_+ - \lambda_-)^{-1}[e^{-\lambda_- t} - e^{-\lambda_+ t}], \end{aligned} \tag{3}$$

where the two decay components are given by

$$\lambda_{\pm}=\tfrac{1}{2}\{(K_1+K_2+K_{-2}+K_3)\pm[(K_1+K_2-K_{-2}-K_3)^2 + 4K_2K_{-2}]^{1/2}\}. \quad (4)$$

In the present case, $(K_2-K_{-2})\gg(K_1-K_3)$ because of the long radiative lifetimes as well as the absence of appropriate exit channels for the low-lying vibrational levels of the $^3B_1$ state. Thus, the second term of Eq. (4) can be approximated as

$$[(K_1+K_2-K_{-2}-K_3)^2+4K_2K_{-2}]^{1/2}\approx K_2+K_{-2}. \quad (5)$$

Then, the decay constants can be expressed as

$$\begin{aligned}\lambda_+ &\cong (K_2+K_{-2})+\tfrac{1}{2}(K_1+K_3)\\ &=[(k^{10}+k^{01})+\tfrac{1}{2}(k^{Q1}+k^{Q0})][\mathrm{SO_2}]+\frac{1}{2}\left(\frac{1}{\tau_1}+\frac{1}{\tau_0}\right),\\ \lambda_- &\cong \tfrac{1}{2}(K_1+K_3)=\tfrac{1}{2}(k^{Q1}+k^{Q0})][\mathrm{SO_2}]+\frac{1}{2}\left(\frac{1}{\tau_1}+\frac{1}{\tau_0}\right).\end{aligned} \quad (6)$$

Now the physical meanings of the slopes and intercepts obtained from Fig. 5 can be interpreted from Eq. (6). It is clear that the zero pressure intercepts for the fast and slow components should be the same and they are the average value of the effective lifetime of the coupled levels. It is noteworthy that the slope of the fast component is given by the sum of the vibrational relaxation/mixing rate constants and the average value of the purely quenching rate constants of the two levels. The latter is also obtained from the slope of the slow component. When the effective radiative lifetime and purely quenching rate constants measured from the $^3B_1(0,0,0)$ level are used, it is found that the effective radiative lifetimes and quenching rate constants for both levels are virtually the same. Finally, the detailed vibrational relaxation/mixing rate constants are obtained using the equilibrium constant expression

$$K_{\mathrm{eq}}=k^{01}/k^{10}=(g_{010}/g_{000})\exp(-\Delta E/kT). \quad (7)$$

Since the ratio of the degeneracies is 1, the rate constants in pure SO_2 are

$$\begin{aligned}&k^{10}=(2.3\pm0.1)\times10^{-11}\ \ \mathrm{cm^3\,molecule^{-1}\,s^{-1}},\\ &k^{01}=(4.0\pm0.2)\times10^{-12}\ \ \mathrm{cm^3\,molecule^{-1}\,s^{-1}},\\ &k^{Q1}\approx k^{Q0}=(6.7\pm0.2)\times10^{-13}\ \ \mathrm{cm^3\,molecule^{-1}\,s^{-1}},\\ &\tau_1\approx\tau_0=(0.6\pm0.1)\ \ \mathrm{ms}.\end{aligned} \quad (8)$$

The validity of this set of rate constants is tested by kinetic simulations of the time profiles at different pressures. The experimental time profiles from the $^3B_1(0,0,0)$ and $^3B_1(0,1,0)$ excitations, respectively, at three different SO_2 pressures are plotted in Fig. 6 with circles and triangles. Although the experimental time profiles include 512 data points, only one-tenth of the experimental data points were plotted in Fig. 6 for clarity. In addition, the magnification factors for the relative intensities of $^3B_1(0,1,0)$ emissions are shown in Figs. 6(a)–6(c). When the $^3B_1(0,0,0)$ level was excited at 388.3 nm, weak emissions from the $^3B_1(0,1,0)$ level were observed as shown in Figs. 6(a)–6(c). The rising part of the emissions from the $^3B_1(0,1,0)$ level is clearly time delayed in comparison with that of the laser excited level, which suggests that the molecules in the $^3B_1(0,1,0)$ level are formed by a collisional mixing process.

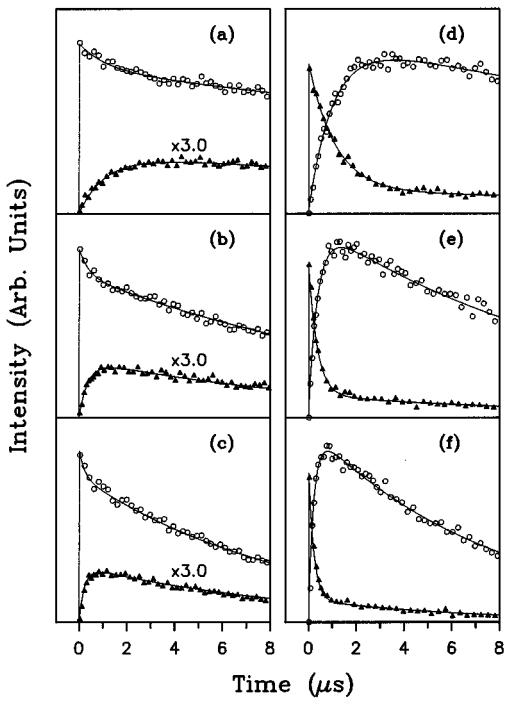

FIG. 6. Comparison of the experimental and calculated time profiles from $^3B_1(0,0,0)$ excitation [(a)–(c)] and $^3B_1(0,1,0)$ excitation [(d)–(f)] at 1.0 [(a),(d)], 3.0 [(b),(e)], and 5.0 Torr [(c),(f)] of SO_2. The magnification factors for the emissions from the $^3B_1(0,1,0)$ level (▲–▲) are shown.

When the $^3B_1(0,1,0)$ level was excited at 382.9 nm, the emissions from the laser excited level decayed quite fast and relatively strong emissions from the $^3B_1(0,0,0)$ level were observed as shown in Figs. 6(d)–6(f). The rise time of the emissions from the $^3B_1(0,0,0)$ level is also clearly time delayed and pressure dependent, which suggests that this level is populated by a collisional process. The shapes of the time profiles from the laser excited and product levels suggest that the vibrational mixing is quite fast. Also noteworthy is the correspondence of the rising part of the collisional product level to the early decaying part of the laser excited level at different pressures.

The solid lines in Fig. 6 are the simulated time profiles using the above rate constants at each pressure. The effective radiative lifetime (0.6 ms) was used to simulate the time profiles shown in Fig. 6, because all the experimental time profiles were obtained through the monochromator. However, the shapes and relative intensities of the simulated time profiles for the laser excited and the product levels using the true radiative lifetime (8.8 ms) were found to be practically the same, because the effective radiative lifetime itself is probably too long to affect the relaxation process. The matching between the experimental and simulated time profiles is good enough to support the above rate constants.

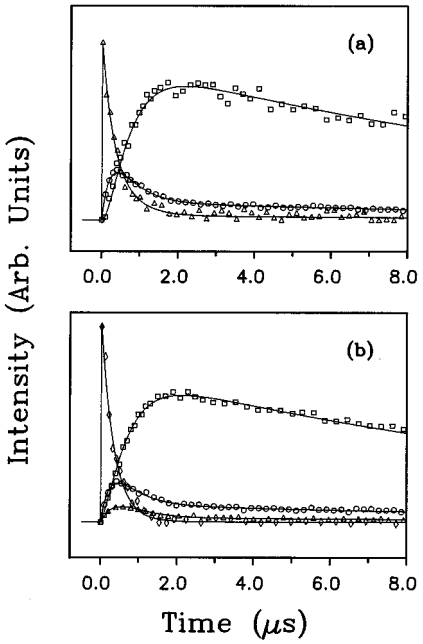

FIG. 7. Comparison of experimental and calculated time profiles at 3.0 Torr of SO_2: (a) $^3B_1(0,2,0)$ excitation and (b) $^3B_1(1,0,0)$ excitation. The different symbols correspond to emissions from the (0,0,0)[□–□], (0,1,0)[○–○], (0,2,0)[△–△], and (1,0,0) levels [◇–◇]. The decay curves from (0,2,0) and (1,0,0) emissions are plotted with 4× magnification.

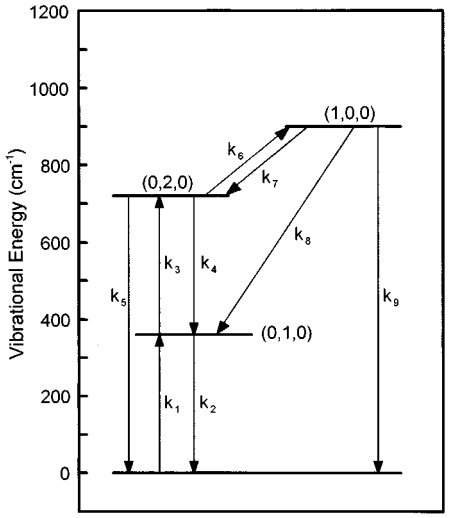

FIG. 8. Low-lying vibrational energy level diagram for the $^3B_1$ state of SO_2, and kinetic scheme for vibrational relaxation.

D. Vibrational relaxation of $^3B_1(0,2,0)$ and $^3B_1(1,0,0)$ levels in SO_2

Fast vibrational relaxation in the $^3B_1$ state is also supported by the results from the $^3B_1(0,2,0)$ and $^3B_1(1,0,0)$ level excitations in SO_2. When the $^3B_1(0,2,0)$ level was pumped at 377.7 nm, it was found that the $^3B_1(0,2,0)\rightarrow{}^1A_1(1,1,0)$ emissions at 408.5 nm were well isolated from other bands even though its intensity was weak. On the other hand, the $^3B_1(1,0,0)\rightarrow{}^1A_1(1,0,0)$ peak at 392.0 nm was also well isolated from others when the $^3B_1(1,0,0)$ level was pumped at 375.1 nm. Thus, the time behavior of the laser excited level could be investigated by monitoring the emissions at these wavelengths. The time profiles from the $^3B_1(0,2,0)$ and $^3B_1(1,0,0)$ levels monitored at 408.5 and 392.0 nm, respectively, following laser excitation at 377.7 and 375.1 nm, also appeared to be a double exponential decay. However, the amplitude of the slow component was too weak for a reliable analysis. Thus, the decay curves were fitted to a single exponential function. The apparent quenching rate constants obtained from the Stern–Volmer plots for these levels are also compiled in Table I. They are virtually the same magnitude as those for the $^3B_1(0,1,0)$ level.

When either the $^3B_1(0,2,0)$ or $^3B_1(1,0,0)$ level was pumped at 377.7 or 375.1 nm, relatively strong emissions from the $^3B_1(0,1,0)$ and $^3B_1(0,0,0)$ levels always appeared with a time delay and the emissions from the laser excited level decayed fast. Typical shapes of the time profiles for the laser excited and product levels are shown in Fig. 7, which were taken at 3.0 Torr. To obtain more information on the state-to-state rate constants, kinetic simulations were attempted based on the kinetic scheme shown in Fig. 8. Since no spectroscopic information is available yet for the asymmetric vibrational mode of the $^3B_1$ state, the $^3B_1(0,0,1)$ level was not included in the kinetic scheme. The solid lines show the calculated time profiles by assigning appropriate fractions of the experimentally obtained quenching rate constants to each process in the kinetic scheme, and the state-to-state rate constants for the best fits are shown in Table II.

E. Quenching of the $^3B_1$ state by other gases

We have also investigated the quenching rate constants for the $^3B_1(0,0,0)$ and $^3B_1(0,1,0)$ levels of SO_2 by Ar, N_2, O_2, and CO_2. The SO_2 pressure in the phosphorescence cell was

TABLE II. Vibrational mixing and relaxation rate constants of a $^3B_1$ state of SO_2 by different quenching gases.

Process	Collision partner	Rate constants (10^{-11} cm^3 molecule^{-1} s^{-1})
$^3B_1(0,0,0)+M\rightarrow{}^3B_1(0,1,0)+M$	SO_2	0.4 (k_1)
	Ar	0.04
	N_2	0.09
	O_2	0.08
	CO_2	0.2
$^3B_1(0,1,0)+M\rightarrow{}^3B_1(0,0,0)+M$	SO_2	2.3 (k_2)
	Ar	0.26
	N_2	0.48
	O_2	0.50
	CO_2	1.3
$^3B_1(0,1,0)+M$ $\rightarrow{}^3B_1(0,2,0)+M$	SO_2	0.4 (k_3)
$^3B_1(0,2,0)+M$		
$\rightarrow{}^3B_1(0,1,0)$		2.6 (k_4)
$\rightarrow{}^3B_1(0,0,0)+M$	SO_2	$\leqslant$0.04(k_5)
$\rightarrow{}^3B_1(1,0,0)$		0.16(k_6)
$^3B_1(1,0,0)+M$		
$\rightarrow{}^3B_1(0,2,0)$		0.40(k_7)
$\rightarrow{}^3B_1(0,1,0)+M$	SO_2	2.1 (k_8)
$\rightarrow{}^3B_1(0,0,0)$		0.50(k_9)

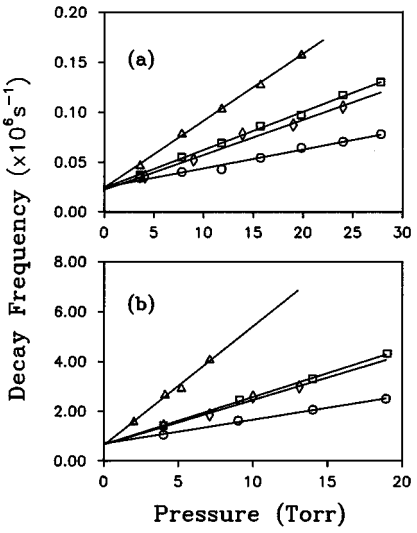

FIG. 9. The pressure dependence of decay constants for (a) $^3B_1(0,0,0) \rightarrow {}^1A_1(1,1,0)$ and (b) fast component of $^3B_1(0,1,0) \rightarrow {}^1A_1(1,0,0)$ emissions by Ar(○–○), O_2 (◇–◇), N_2 (□–□), and CO_2 (△–△). The SO_2 pressure was kept constant at 1.0 Torr and quenching gases were added. The zero pressure intercepts are much different from each other because of the efficient quenching by SO_2 for the $^3B_1(0,1,0)$ level.

kept constant at 1.0 Torr for these experiments, and the quenching gases were added to the cell. All the time profiles from the $^3B_1(0,0,0)$ level excitation monitored at 415.5 nm showed a single exponential decay. The pressure dependence of the decay frequencies is plotted in Fig. 9(a), and the quenching rate constants are also shown in Table I.

When the $^3B_1(0,1,0)$ level was pumped, all the time profiles from the laser excited level showed a double exponential decay as in pure SO_2. Indeed, the pressure dependence of the decay frequencies of the slow components was virtually the same as that shown in Fig. 9(a), as expected from the experimental results in pure SO_2. The Stern–Volmer plots for the fast components are shown in Fig. 9(b), and the slopes for the fast and slow components are also shown in Table I. The vibrational relaxation/mixing rate constants for the $^3B_1(0,1,0)$ level by Ar, N_2, O_2, and CO_2 are also obtained using the slopes of the fast and slow components and the detailed balance. The results are shown in Table II.

IV. DISCUSSION

The radiative lifetime of the $^3B_1$ state of SO_2 in the gas phase had been a subject of interest until the mid 1970's, because the experimentally measured values appeared much shorter than the calculated one (12.6 ± 0.8 ms) from the integrated absorption coefficient.[1,5–10] Calvert and co-workers[9(a)] finally obtained 8.1 ± 2.5 ms for the radiative lifetime of the $^3B_1$ state, and it has been accepted as the best experimental value. They employed a large 22 l bulb and generated the $^3B_1$ state of SO_2 by pumping at 363.1 nm. In this work, we have generated the $^3B_1(0,0,0)$ level by exciting at 388.3 nm in a 2 l bulb and obtained 8.8 ± 2.5 ms, which is in good agreement with that of Calvert and co-workers.[9(a)] Since the quenching of the $^3B_1(0,0,0)$ level by Ar was found to be much slower than that by SO_2, we have also investigated the radiative lifetime of the $^3B_1(0,0,0)$ level using 1.0% SO_2 in Ar. The Stern–Volmer plots for 1.0–10.0 Torr of this mixed gas also gave the same zero pressure intercepts. Thus we have confirmed that the radiative lifetime of the $^3B_1$ state is very long and close to that obtained from the integrated absorption coefficient.

The excitation wavelengths to populate a specific vibrational level in this work match well with those peak positions of the corresponding absorption bands reported by Wampler and co-workers,[18] and they are not overlapping each other. Although the radiative lifetime of the SO_2 molecules in the $^3B_1$ state is very long, it was possible to monitor the time behavior of the vibrationally excited molecules in the $^3B_1$ state using a monochromator due to the relatively fast relaxation processes. Since the observation wavelengths for the emissions from the vibrationally excited level were chosen from the time resolved spectra, the time profiles observed through the monochromator for each level were not contaminated by emissions from other levels.

The collisional quenching of the $^3B_1$ state in SO_2 has been studied in many laboratories.[8–10] The quenching rate constant for the $^3B_1(0,0,0)$ level in the present work is in good agreement with the previously reported values, although the initial species generated in most of the previous works were not those in the lowest vibrational level of the $^3B_1$ state. This is easily understood considering the fast vibrational relaxation in the $^3B_1$ state and the long radiative lifetime of those species. The prominent peaks observed in the typical phosphorescence spectra from the $^3B_1$ state of the SO_2 molecules, which appear in the 380–450 nm region are, in fact, those emissions for $X\ {}^1A_1(\nu_1,\nu_2,\nu_3) \leftarrow {}^3B_1(0,0,0)$ transitions as assigned by Brand and co-workers,[12] Hochstrasser and Marchetti,[14] and Carter *et al.*[15] The collisional quenching of the $^3B_1$ state by other gases also has been studied by Calvert and co-workers[9(c)] and Briggs *et al.*,[10] and those values are in agreement with ours within 50% as shown in Table I.

The following types of processes have been suggested as the dominant channels for the collisional quenching of the $^3B_1$ state by the ground state SO_2:

$$^3B_1 + SO_2 \rightarrow 2\ SO_2, \tag{9a}$$

$$^3B_1 + SO_2 \rightarrow SO_3 + SO. \tag{9b}$$

Strickler and Rudolph,[8(b)] Calvert and co-workers,[9(b)] and Wampler and co-workers[19] reported that the magnitude of the reactive quenching rate constant for Eq. (9b) is 12%–13% of the total quenching rate constant. It is difficult to figure out what fractions of the total quenching rate constants are due to the reactive channel in this work. However, it seemed not to be the dominant channel, because we did not observe any discernible decrease in the emission intensities when we pumped the $^3B_1(0,0,0)$ level for several hours in a static condition.

The vibrational relaxation rate constants for the $^3B_1(0,1,0)$ level of the $^3B_1$ state by SO_2, Ar, N_2, O_2, and CO_2 have been determined explicitly from the pressure dependence of the decay constants for the fast and slow compo-

nents in this work. Also, we have assigned the state-to-state relaxation rate constants from the $^3B_1(0,2,0)$ and $^3B_1(1,0,0)$ levels in SO_2 by kinetic simulations of the time profiles. Heicklen and co-workers[1] presented a kinetic model to explain the results of Wampler and co-workers.[20] They suggested that the relaxation rate constants in the $^3B_1$ state would be $\simeq 1.6\times10^{-10}$ cm^3 $molecule^{-1}$ s^{-1}. This value, however, is far larger than the rate constants measured in this work.

Flynn and co-workers[21] studied the $V-V$ transfer rate constants for the ground state of SO_2 and found that the $V-V$ transfer rate is very slow. They excited the (1,0,0) level using a CO_2 laser and observed emissions from the (0,0,1) level. They obtained $k_{13}(\nu_1\rightarrow\nu_3)=8.3\times10^{-13}$ and $k_{12}(\nu_1\rightarrow2\nu_2)=2.1\times10^{-13}$ cm^3 $molecule^{-1}$ s^{-1}, respectively. It is difficult to compare the ground state $V-V$ transfer rate constants with the vibrational relaxation rate constants obtained for the $^3B_1$ state, because we were not able to obtain any informations on the $\nu_1\rightarrow\nu_3$ transfer rate constants in the $^3B_1$ state. Nevertheless, it might be useful for looking at the differences in the dominant vibrational relaxation pathways for both states, when the (1,0,0) level in each state is populated. In the ground state, the rate constant for $\nu_1\rightarrow2\nu_2$ is about 25% of that for $\nu_1\rightarrow\nu_3$, and the rate constant for $\nu_1\rightarrow\nu_2$ may be negligibly small compared to others. In the present study for the $^3B_1$ state, the experimental time profiles for the laser excited as well as the product levels could be fitted by calculated ones by assigning 70% of the total quenching rate constant for $\nu_1\rightarrow\nu_2$, 13% for $\nu_1\rightarrow2\nu_2$, and 17% for the (0,0,0) level. The large branching fractions for the $\nu_1\rightarrow\nu_2$ process could be ascribed to the following near resonance channel:

$$^3SO_2(\nu_1)+{}^1SO_2\rightarrow{}^3SO_2(\nu_2)+{}^1SO_2(\nu_2),$$
$$\Delta E=-22\ \ cm^{-1}. \tag{10}$$

It is not clear whether the large vibrational relaxation rate constants observed for the $^3B_1$ state in this work belong to the $V-V$ or $V-T/R$ process, since the kinetics for an electronically excited state is much more complicated than that for the ground state. Nevertheless, it is interesting that the relaxation rate constant for the $^3B_1(0,1,0)$ level measured in this work matches well with the calculated $V-T/R$ rate constant, 2.3×10^{-11} cm^3 $molecule^{-1}$ s^{-1}, for the (0,1,0) level of the ground state by Revelant and Manzanares I.[22] Although this matching could be fortuitous, it suggests that the magnitudes of our relaxation rate constants are in the reliable range. Moreover, the state-to-state relaxation rate constants from the (0,2,0) and (1,0,0) levels assigned from the kinetic simulations of the time profiles suggest that the fast vibrational relaxation in the $^3B_1$ state may occur through the ν_2 mode.

V. CONCLUSIONS

The vibrational relaxation rate constants for the low-lying vibrational levels in the $a\ ^3B_1$ state of SO_2 have been studied by directly populating these levels from the ground state. The radiative lifetime, 8.8 ± 2.5 ms, for the $^3B_1(0,0,0)$ level is in good agreement with that reported by Su *et al.*[9(a)] It is clearly shown that the quenching rate constants for the $^3B_1$ state previously reported in the literature are those for the $^3B_1(0,0,0)$ level. The apparent quenching rate constants for upper vibrational levels are much larger than that for the $^3B_1(0,0,0)$ level due to the large relaxation rate constants. Because of the long radiative lifetime as well as the relatively large relaxation rate constants, the thermal equilibrium in the $^3B_1$ state is reached in a short time. The vibrational relaxation rate constants in the $^3B_1$ state, however, are an order of magnitude smaller than the gas kinetic rate constant at room temperature. The explicit vibrational relaxation rate constants in the $^3B_1$ state reported in this work will be very useful for reexamining and clarifying those complicated kinetics among the low-lying excited states of SO_2 in the 3.2–4.5 eV region.

ACKNOWLEDGMENTS

This work is financially supported, in part, by the Korea Science and Engineering Foundation through the Center for Molecular Science at KAIST and in part by RIST through their basic science research program.

[1] J. Heicklen, N. Kelly, and K. Partymiller, Rev. Chem. Intermediates **3**, 315 (1980).
[2] J. Heicklen, *Atmospheric Chemistry* (Academic, New York, 1976).
[3] A. E. Douglas, Can. J. Phys. **36**, 147 (1958).
[4] A. J. Merer, Discuss. Faraday Soc. **35**, 127 (1963).
[5] B. P. Levitt and D. P. Sheen, Trans. Faraday Soc. **63**, 540 (1967).
[6] A. McKenzie and B. A. Thrush, Proc. R. Soc. London Ser. A **308**, 133 (1968).
[7] R. B. Caton and A. B. F. Duncan, J. Am. Chem. Soc. **90**, 1945 (1968).
[8] (a) S. J. Strickler, J. P. Vikesland, and H. D. Bier, J. Chem. Phys. **60**, 664 (1974); (b) S. J. Strickler and R. N. Rudolph, J. Am. Chem. Soc. **100**, 3326 (1978); (c) S. J. Strickler and R. D. Ito, J. Phys. Chem. **89**, 2366 (1985).
[9] (a) F. Su, J. W. Bottenheim, D. L. Thorsell, J. G. Calvert, and E. K. Damon, Chem. Phys. Lett. **49**, 305 (1977); (b) K. Chung, J. G. Calvert, and J. W. Bottenheim, Int. J. Chem. Kinet. **7**, 161 (1975); (c) H. W. Sidebottom, C. C. Badcock, G. E. Jackson, J. G. Calvert, G. W. Reinhardt, and E. K. Damon, Environ. Sci. Technol. **6**, 72 (1972); (d) H. W. Sidebottom, C. C. Badcock, J. G. Calvert, G. W. Reinhardt, R. B. Rabe, and E. K. Damon, J. Am. Chem. Soc. **93**, 2587 (1971); (e) K. Otsuka and J. G. Calvert, *ibid.* **93**, 2581 (1971); (f) T. N. Rao, S. S. Collier, and J. G. Calvert, *ibid.* **91**, 1609 (1969).
[10] J. P. Briggs, R. B. Caton, and M. J. Smith, Can. J. Chem. **53**, 2133 (1975).
[11] K. Kamiya and H. Matsui, Bull. Chem. Soc. Jpn. **64**, 2792 (1991).
[12] J. C. D. Brand, V. T. Jones, and C. D. Lauro, J. Mol. Spectrosc. **45**, 404 (1973).
[13] F. Su, J. W. Bottenheim, H. W. Sidebottom, G. A. Calvert, and E. K. Damon, Int. J. Chem. Kinet. **10**, 125 (1978).
[14] R. M. Hochstrasser and A. P. Marchetti, J. Mol. Spectrosc. **35**, 335 (1970).
[15] S. Carter, I. M. Mills, J. N. Murrell, and A. J. C. Varandas, Mol. Phys. **45**, 1053 (1982).
[16] J. T. Yardley, *Introduction to Molecular Energy Transfer* (Academic, New York, 1980).
[17] G. Inoue, J. K. Ku, and D. W. Setser, J. Chem. Phys. **80**, 6006 (1984).
[18] F. B. Wampler, R. C. Oldenborg, and W. W. Rice, J. Appl. Phys. **50**, 6117 (1979).
[19] F. B. Wampler, R. C. Oldenberg, W. W. Rice, and R. R. Karl, Jr., J. Chem. Phys. **69**, 2569 (1978).
[20] F. B. Wampler, K. Otsuka, G. J. Calvert, and E. K. Damon, Int. J. Chem. Kinet. **5**, 669 (1973).
[21] (a) D. Siebert and G. W. Flynn, J. Chem. Phys. **62**, 1212 (1975); (b) B. L. Earl, A. M. Ronn, and G. W. Flynn, Chem. Phys. **9**, 307 (1975); (c) G. A. West, R. E. Weston, Jr., and G. W. Flynn, J. Chem. Phys. **67**, 4873 (1977).
[22] V. Revelant and C. Manzanares I, Chem. Phys. **69**, 473 (1982).